Tuberculosis

International Edition: DOI: 10.1002/anie.201505493
German Edition: DOI: 10.1002/ange.201505493

Isoniazid@Fe_2O_3 Nanocontainers and Their Antibacterial Effect on Tuberculosis Mycobacteria

Peter Leidinger, Jens Treptow, Kristine Hagens, Jacqueline Eich, Nicole Zehethofer, Dominik Schwudke, Wulf Oehlmann, Heinrich Lünsdorf, Oliver Goldmann, Ulrich E. Schaible, Kurt E. J. Dittmar,* and Claus Feldmann**

Dedicated to Professor Ulrich Müller on the occasion of his 75th birthday

Abstract: *Isoniazid-filled Fe_2O_3 hollow nanospheres (INH@Fe_2O_3, diameter <30 nm, 48 wt% INH-load) are prepared for the first time and suggested for tuberculosis therapy. After dextran-functionalization, the INH@Fe_2O_3@DEX nanocontainers show strong activity against Mycobacterium tuberculosis (M.tb.) and M.tb.-infected macrophages. The nanocontainers can be considered as "Trojan horses" and show efficient, active uptake into both M.tb.-infected macrophages and even into mycobacterial cells.*

Tuberculosis (TB)—according to the World Health Organization (WHO)—is one of the most prevalent infectious diseases worldwide causing high mortality. In 2013, around 9 million TB cases and 1.5 million mortalities were reported.[1] TB has regained tremendous attention owing to its deadly liaison with HIV as well as due to the alarming emergence of multidrug resistant (MDR) and extremely drug resistant (XDR) isolates.[1,2] Notably, about one third of the world's population is estimated to be latently infected, with a 10% chance to become active during life time. The pathogenic agent, *Mycobacterium tuberculosis* (*M.tb.*), resides as facultative intracellular parasite in macrophages encapsulated in granulomas.[3] Therefore, therapy, especially of latent TB, remains a big challenge.[1,3]

[*] Dr. P. Leidinger, J. Treptow, Prof. Dr. C. Feldmann
Institut für Anorganische Chemie
Karlsruhe Institute of Technology (KIT)
Engesserstrasse 15, 76131 Karlsruhe (Germany)
E-mail: claus.feldmann@kit.edu
K. Hagens, J. Eich, Dr. N. Zehethofer, Dr. D. Schwudke, Prof. Dr. U. E. Schaible
Forschungszentrum Borstel, Leibniz-Zentrum für Medizin und Biowissenschaften, Priority Area Infections
Parkallee 1–40, 23845 Borstel (Germany)
E-mail: uschaible@fz-borstel.de
Dr. W. Oehlmann
Lionex—Diagnostics and Therapeutics GmbH
Salzdahlumer Strasse 196, 38126 Braunschweig (Germany)
Dr. H. Lünsdorf, Dr. O. Goldmann, Dr. K. E. J. Dittmar
Helmholtz-Zentrum für Infektionsforschung
Inhoffenstrasse 7, 38124 Braunschweig (Germany)
E-mail: kurt.dittmar@helmholtz-hzi.de

Supporting information for this article is available on the WWW under http://dx.doi.org/10.1002/anie.201505493.

In principle, efficient antibiotics, such as isoniazid (isonicotinylhydrazine, INH), rifampicin (RIF), pyrazinamide (PYZ), or ethambutol (ETB) are available for TB therapy.[2,4] However, anti-mycobacterial drugs have not only to cross the granuloma encapsulation and the host macrophage membrane but also the lipid-rich cell wall of the mycobacterial cell. Additional restrictions are related to the limited permeability into biofilms of the drugs and their rapid degradation in the physiological environment at low dose, but heavy side-effects at higher doses.[2,4] TB therapy requires daily taking of doses up to 5 mg kg^{-1} of body weight for 6–9 months. Typical side effects include, hepatitis, anemia, seizures, renal failure, ataxia, or allergenic hypersensitivity. As a result of the reduced quality of life, patients however, tend to abandon their therapy, which is the main reason of bacterial multi-resistances.[2–5]

In view of the above considerations, affordable and efficient TB agents and their administration are needed to decrease the dose, shorten the therapy's duration, and minimize/avoid side effects. This will increase patient's compliance and minimize the risks of therapy failure and bacterial resistance.[1–5] Nanomaterials, in general, have already offered promising strategies to molecular biology and medicine. Hence, their use for advanced imaging techniques[6] and cancer therapy has been intensely investigated in recent years.[7] For TB treatment, efficient shuttle systems to infiltrate infected cells with antibiotics are highly desired. Such shuttles should contain a high load of antibiotics, and they need to be biocompatible, biodegradable, and optimally excreted residue-free after 2–3 days.[8] However, nanomaterials for TB treatment have been rarely considered to date.[9] Thus far, SiO_2[10] and polymer[11] nanoparticles have been coated or loaded with TB antibiotics. In addition, the intrinsic antibacterial activity of nanoscaled silver has been used.[12] Most often, these studies address comparably large particles (>50 nm) with limited load of antibiotics (<10 wt%).

As a new strategy, we suggest isoniazid-filled iron oxide nanocontainers (INH@Fe_2O_3) for TB therapy. The INH@Fe_2O_3 nanocontainers were synthesized by a modified microemulsion approach (Figure 1).[13] Thus, a reversed microemulsion was established with *n*-dodecane as the non-polar dispersant phase, hexadecyltrimethylammonium bromide (CTAB) as the surfactant, *n*-hexanol as the co-surfactant and diluted H_2O_2 (1.4 vol%) as the polar phase. INH was

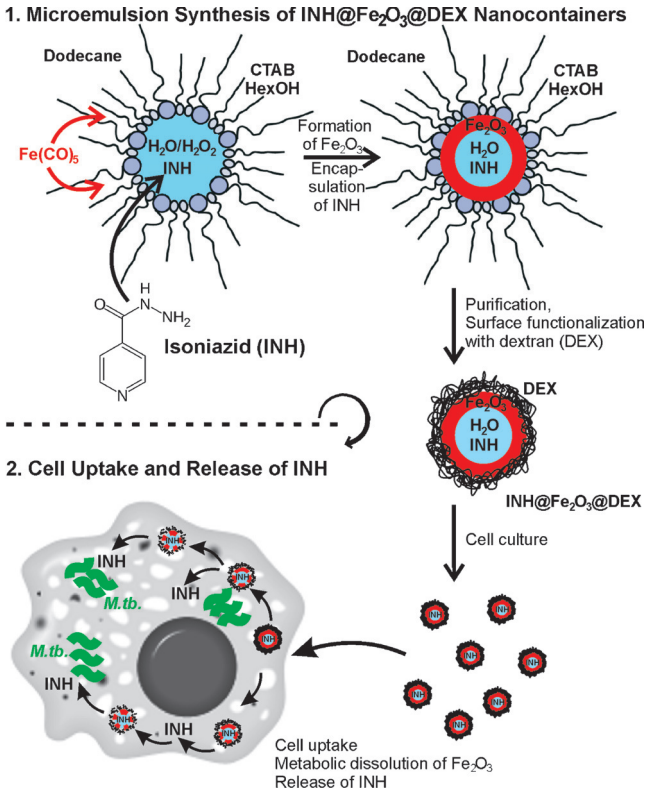

Figure 1. The microemulsion synthesis, dextran functionalization, uptake of INH@Fe_2O_3@DEX nanocontainers, and INH-release in *M.tb.*-infected macrophages.

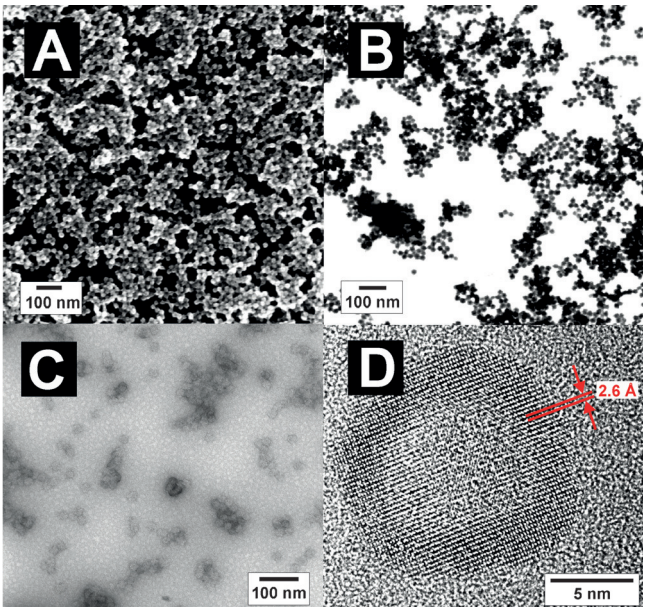

Figure 2. Particle size and size distribution of INH@Fe_2O_3 nanocontainers according to electron microscopy at different levels of magnification: A) SEM, B) STEM, C),D) HRTEM.

added to the water phase, whereas $Fe(CO)_5$ was added to the dodecane phase of the microemulsion. Thereafter, H_2O_2-driven room-temperature oxidation of $Fe(CO)_5$ resulted in a slow formation of brownish Fe_2O_3. Since $Fe(CO)_5$ and H_2O_2 were dissolved in different phases, their reaction is limited to the micelle's liquid-to-liquid phase boundary. As a result, the INH-containing water droplet is encapsulated by Fe_2O_3 forming INH@Fe_2O_3 nanocontainers (Figure 1). Since $Fe(CO)_5$ is the stronger reducing agent, oxidation of INH is prevented and H_2O_2 completely consumed by reaction with $Fe(CO)_5$ (Supporting Information: Figures S1–S3).

Electron microscopy (SEM, STEM, HRTEM) confirms a uniform, spherical morphology of the INH@Fe_2O_3 nanocontainers (Figure 2). Statistical evaluation of 100 particles results in a mean diameter of 18(1) nm (Figure 2A,B; Figure S1A). STEM and HRTEM images reveal the structure of the nanocontainers with an outer diameter of 15–20 nm, a wall thickness of 2–4 nm, and an inner cavity diameter of 8–10 nm (Figure 2C,D). HRTEM, furthermore, indicates the crystallinity of the sphere wall with lattice distances of 2.6 Å (bulk-γ-Fe_2O_3/maghemite: $d(311) = 2.52$ Å) (Figure 2D).[14]

The chemical composition of the INH@Fe_2O_3 nanocontainers was validated based on infrared spectroscopy (FT-IR), thermogravimetry (TG), mass spectrometry (MS), elemental analysis (EA), X-ray powder diffraction (XRD), electron-energy loss spectroscopy (EELS), and energy-dispersive X-ray (EDX) analysis. FT-IR and MS show the characteristic fingerprint vibrations and mass peaks of INH (Figure S2). The presence of Fe_2O_3 was confirmed by HRTEM (Figure 2D), EDX, XRD, and EELS (Figures S3,S4,S6,S7). The INH-load of the nanocontainers was quantified by TG (Figure S3). Thus, the nanocontainers consist of 9 wt% of water, 48 wt% of INH in the inner cavity, and 43 wt% of Fe_2O_3 as the sphere wall. At about half of the total weight, the INH-load is significantly higher in comparison to known nanoparticle concepts for TB therapy.[9–12] To improve membrane permeability and cell uptake, the as-prepared INH@Fe_2O_3 nanocontainers were functionalized with dextran (DEX) and redispersed in isotonic water (Figure 1).[15] In this step, sephadex as a crosslinked, high molecular-weight dextran derivative was used (Supporting Information). The resulting INH@Fe_2O_3@DEX nanocontainers exhibit a mean hydrodynamic diameter of 26(2) nm as a result of DEX functionalization (Figure S1B,C,S5).

Biocompatibility and cell uptake of the INH@Fe_2O_3@DEX nanocontainers were verified in vitro by feeding them to mammalian cells (i.e., murine bone-marrow-derived macrophages, immature human dendritic cells, Supporting Information). These cells generally show a high uptake rate of nanoparticles and a fast response to putatively toxic compounds.[16] Both cell types show normal viability and proliferation rates upon internalization of INH@Fe_2O_3@DEX. The response of the macrophages was quantified based on reactive oxygen species (ROS), inducible nitric oxide (iNOs), and released lactate dehydrogenase (LDH) (Figure S8,S9). Although substantial ROS formation was as expected induced by the Fe-content of the nanoparticles,[17] low levels of NO and LDH indicate a sufficient biocompatibility of the INH@Fe_2O_3@DEX nanocontainers. ROS formation in absence of cytotoxic effects, in fact, can add another antimicrobial advantage for combating TB as it

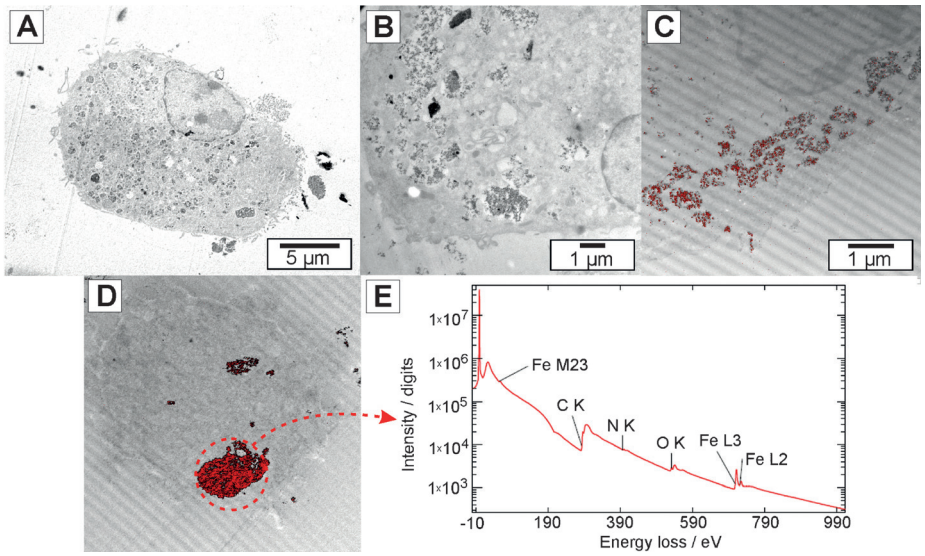

Figure 3. Cell uptake of INH@Fe_2O_3@DEX nanocontainers: A) Low- and B) high-resolution images of nanocontainer-treated macrophages; C),D) Vesicles overlaid with Fe-*L23* elemental map indicating INH@Fe_2O_3@DEX as red dots; E) WR-PEEL spectra of nanocontainer agglomerate (red circle in (D)).

affects mycobacterial viability, activates cells, and immunostimulates cytokine secretion.[3,18]

To demonstrate uptake of the nanocontainers by macrophages, cells grown on a plastic surface were fixed and cut "en face" in parallel sections. Electron micrographs show that the cytoplasm of the nanocontainer-treated macrophages is enriched with electron-opaque clusters showing characteristic electron-dense granular substructures (Figure 3 A,B). Hence, the nanocontainers are exclusively localized in vesicles. Parallel electron-energy loss (PEEL) spectra of INH@Fe_2O_3@DEX-containing vesicles clearly show the ionization onsets of Fe-*M23*/*L23* and confirm the presence of iron in the granular structures (Figure 3 C–E). The INH@Fe_2O_3@DEX nanocontainers within vesicles colocalize by overlay with an Fe-*L23* elemental map (Figure 3 C,D). Statistical analysis of cell intersections, revealed a mean of 1400 nanocontainers per cell (Table S1). This high-nanocontainer uptake by macrophages fulfills the requirement to access intracellular mycobacteria located after phagocytosis in macrophages phagosomes.[2–5]

The activity of INH@Fe_2O_3@DEX nanocontainers was tested on *M.tb.* cultures (strain H37Rv, handling of *M.tb.* requires biosafety level 3 equipment, Supporting Information). Different concentrations of INH@Fe_2O_3@DEX nanocontainers, Fe_2O_3@DEX reference, INH alone, and control medium were tested for activity against *M.tb.* using a resazurin assay biokit measuring mycobacterial metabolism (Figure 4 A) as well as a colony forming unit (CFU) assay assessing viable mycobacterial numbers (Figure 4 B). In both tests, INH alone shows antibacterial activity even at lowest concentration (1 µg mL^{-1}), which is expected since INH has direct access to mycobacteria. The INH-free Fe_2O_3@DEX reference does not show any effect proving general biocompatibility (Figure 4). In contrast, the INH@Fe_2O_3@DEX nanocontainers inhibit metabolic activity and kill *M.tb.* already at INH concentrations as low as 8 µg mL^{-1} (Figure 4). Similar to the well-established slow and complete dissolution of massive iron oxide nanoparticles under physiological conditions along with concurrent ferretin formation,[17,19] INH is clearly released with advancing nanocontainer dissolution. These specific features of iron oxide—biocompatibility, biodegradability, slow dissolution[20]—are used in our nanocontainer concept as well.

After revealing biocompatibility, cellular uptake and activity against mycobacteria, *M.tb.*-infected macrophages were treated with INH@Fe_2O_3@DEX nanocontainers. On TEM images, *M.tb.* mycobacteria are clearly visible within phagosomes inside macrophages (Figure 5 A–C). The characteristic dark, granular structures—similar to Figure 3 A,B—indicate the presence of electron-dense INH@Fe_2O_3@DEX nanocontainers at different states of dissolution (Figure 5 D,E). Often, the nanocontainers are located within a submicron distance of *M.tb.* cells (Figure 5 A–C). This observation may indicate active acquisition of iron by mycobacteria as an essential micro-

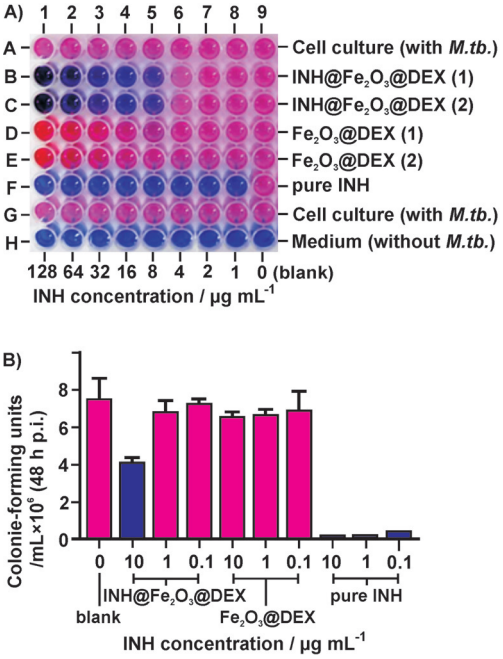

Figure 4. Activity of INH@Fe_2O_3@DEX nanocontainers: A) Resazurin assay indicating *M.tb.* (H37Rv) viability. Orange-red: *M.tb.* positive/active metabolism. Dark blue: *M.tb.* negative/metabolism aborted. B) Growth of *M.tb.* (references: INH-free Fe_2O_3@DEX, pure INH, blank. INH corresponds to 48 wt% of total INH@Fe_2O_3@DEX weight).

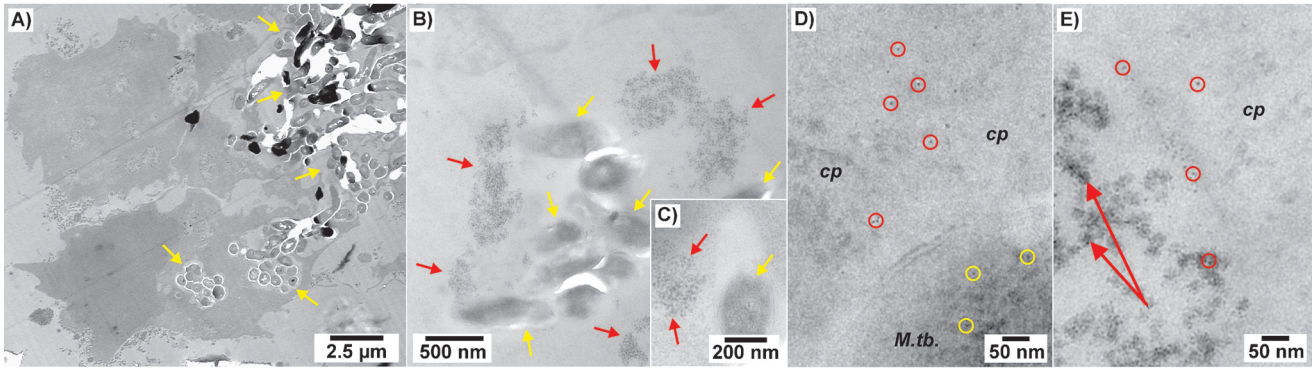

Figure 5. Ultrastructural analysis of *M.tb.*-infected macrophages treated with INH@Fe_2O_3@DEX nanocontainers: A) TEM (90 nm section) with *M.tb.*-infected macrophages with B,C) INH@Fe_2O_3@DEX (red arrows) in the immediate vicinity of bacterial cells (yellow arrows). D) Detailed view of INH@Fe_2O_3@DEX-treated macrophages, infected with *M.tb.* The macrophage cytoplasm (*cp*) as well as the *M.tb.* cytoplasm contain debris of nanocontainers (red circles: inside macrophages; yellow circles: inside *M.tb.* cells). E) Detailed view of a cluster of INH@Fe_2O_3@DEX nanocontainers (red arrows) in the macrophage cytoplasm (*cp*), associated with nanocontainer debris (red circles). Ultrathin sections in (A,B) show some cracks/holes arising from inhomogeneous resin infiltration/polymerization, caused by interference of the biomatrix.

nutrient for growth and virulence.[21] In fact, it has already been suggested that addressing the mycobacterial iron metabolism could be an efficient TB therapy.[21] The electron microscopy demonstrates that INH@Fe_2O_3@DEX nanocontainers can be considered as "Trojan horses" for antibiotics. HRTEM images show nanocontainers and particulate debris thereof even inside mycobacterial cells (Figure 5D; Figure S10).

The dissolution of the INH@Fe_2O_3@DEX nanocontainers inside the macrophage cytoplasma and outside of the macrophages can be visualized by TEM images and EELS (Figure 6; Figure S11). After overnight cultivation, electron absorption, and Fe-*L23* elemental maps clearly indicate a lower content of iron in intracellular nanocontainers than in extracellular nanocontainers. This finding indicates a preferred dissolution of internalized INH@Fe_2O_3@DEX nanocontainers and confirms the use of iron for macrophage metabolism.[21] In contrast to internalized nanocontainers, INH-release from INH@Fe_2O_3@DEX nanocontainers in physiological media turned out to be very slow (Table S2, Figure S12), which further supports an active acquisition of iron by the macrophages and mycobacteria.

In summary, INH@Fe_2O_3@DEX nanocontainers are a new type of hollow nanospheres with diameters less than 30 nm that can serve as efficient drug-delivery systems for antibiotic TB therapy. With 48 wt% INH, they contain a considerably higher drug load than that offered by alternative nanocontainer concepts. Biocompatibility, biodegradability, and active iron acquisition by infected macrophages and mycobacteria are additional assets of the Fe_2O_3-based nanocontainers. Thus, INH@Fe_2O_3@DEX combines both low cellular toxicity of the nanocontainers and high activity of the encapsulated INH. Acting like a "Trojan horse", the nanocontainers are actively internalized into macrophages and release INH in close proximity to the mycobacteria upon slow metabolic dissolution of the Fe_2O_3 wall, putatively exploiting the mycobacteria's need for iron. Preparation of the nanocontainers as an aerosol-type formulation and in vivo studies are needed as follow-up before they

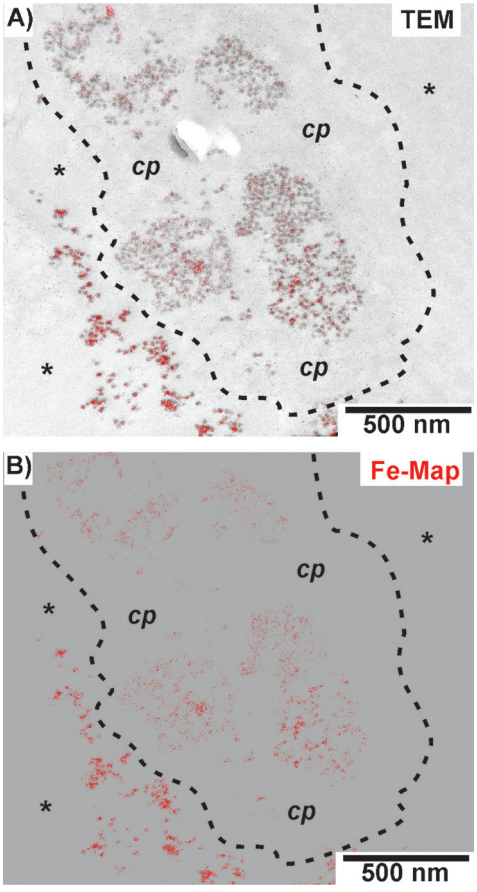

Figure 6. INH@Fe_2O_3@DEX nanocontainers after overnight cultivation at different rates of dissolution inside the macrophage cytoplasma (*cp*) and outside (*) the macrophages (black line indicates cell membrane): A) Overlay of TEM image and Fe-*L23* elemental map; B) Fe-*L23* elemental map from (A).

can be used to directly treat lung tuberculosis and to validate reduced side effects of the new nanocontainer concept. Besides the potential for TB therapy, this concept, synthesis

strategy, and type of nanocontainer may also be relevant for encapsulation, transport, and release of other antibiotics and drugs for unrelated targets, such as virus-infected cells or tumor cells.

Experimental Section

Synthesis**:** In general, the INH@Fe_2O_3@DEX nanocontainers and the INH-free Fe_2O_3@DEX reference were prepared by a modified microemulsion approach following our strategy for preparing hollow nanospheres (e.g., Ag, Au, AlO(OH), SnO_2, $La(OH)_3$, Cu_2S, CuS, Ag_2S) reported elsewhere.[13] A detailed procedure for INH@Fe_2O_3 and INH@Fe_2O_3@DEX is given in the Supporting Information.

Further details of the synthesis, materials characterization, in vitro studies with macrophages, assays, and cell tests with virulent *M.tb.* are described in the Supporting Information.

Acknowledgements

We acknowledge the Bundesministerium für Wirtschaft und Technologie (BMWi) for funding within the project *"Allergie-relevante Analytik mit Nano-Reagenzien (nanoARA)"*. P.L. and C.F. thank Dr. R. Popescu and Prof. Dr. D. Gerthsen (KIT) for TEM analysis and the Deutsche Forschungsgemeinschaft (DFG) for funding of equipment. D.S., N.Z., and U.S. acknowledge the Deutsche Zentrum für Infektionsforschung for funding.

Keywords: in vitro studies · isoniazid · mycobacteria · nanocontainers · tuberculosis

How to cite: *Angew. Chem. Int. Ed.* **2015**, *54*, 12597–12601
Angew. Chem. **2015**, *127*, 12786–12791

[1] World Health Organization (WHO), *Global tuberculosis report 2014*, ISBN 978 92 4 156480 9.
[2] a) *Tuberculosis: A comprehensive clinical reference* (Eds.: H. S. Schaaf, A. Zumla), Saunders Elsevier, Amsterdam, **2009**; b) D. L. Kasper, A. S. Fauci, *Harrison's Infectious Diseases*, McGraw-Hill, New York, **2010**.
[3] Review: G. Weiss, U. Schaible, *Immunol. Rev.* **2015**, *264*, 182.
[4] Reviews: a) A. Zumla, P. Nahid, S. T. Cole, *Nat. Rev. Drug Discovery* **2013**, *12*, 388; b) R. Beena, D. S. Rawat, *Med. Res. Rev.* **2013**, *33*, 693.
[5] Reviews: a) C. Lu, Q. Liu, A. Sarm, C. Fitzpatrick, D. Falzon, C. D. Mitnick, *PloS one* **2013**, *8*, e56074; b) T. Gumbo, *Nat. Genet.* **2013**, *45*, 720.
[6] Reviews: a) S. Chapman, M. Dobrovolskaia, K. Farahani, A. Goodwin, A. Joshi, H. Lee, T. Meade, M. Pomper, K. Ptak, J. Rao, et al., *Nano Today* **2013**, *8*, 454; b) J. G. Fujimoto, D. Farkas, *Biomedical Optical Imaging*, Oxford University Press, Oxford, **2009**.
[7] Reviews: a) C. Li, *Nat. Mater.* **2014**, *13*, 110; b) D. Ling, M. J. Hackett, T. Hyeon, *Nat. Mater.* **2014**, *13*, 122; c) Y. Ding, S. Li, G. Nie, *Nanomedicine* **2013**, *8*, 1209; d) K. Riehemann, S. W. Schneider, T. A. Luger, B. Godin, M. Ferrari, H. Fuchs, *Angew. Chem. Int. Ed.* **2009**, *48*, 872; *Angew. Chem.* **2009**, *121*, 886.
[8] a) M. E. Davis, *Mater. Res. Soc. Bull.* **2012**, *37*, 828; b) J. B. Hall, M. A. Dobrovolskaia, A. K. Patri, S. E. McNeil, *Nanomedicine* **2007**, *2*, 789.
[9] a) F. Fenaroli, D. Westmoreland, J. Benjaminsen, T. Kolstad, F. M. Skjeldal, A. H. Meijer, M. van der Vaart, L. Ulanova, N. Roos, B. Nystrom, *ACS Nano* **2014**, *8*, 7014; b) L. A. Aranha, A. J. Almeida, L. M. D. Goncalves, *J. Biomed. Nanotechnol.* **2014**, *10*, 2295; c) G. Griffiths, B. Nystroem, S. B. Sable, G. K. Khuller, *Nat. Rev. Microbiol.* **2010**, *8*, 827; d) A. Sosnik, A. M. Carcaboso, R. J. Glisoni, M. A. Moretton, D. Chiappetta, *Adv. Drug Delivery Rev.* **2010**, *62*, 547.
[10] a) P. Pedrosa, B. Veigas, D. Machado, I. Couto, M. Viveiros, P. V. Baptista, *Tuberculosis* **2014**, *94*, 332; b) B. Zargar, A. Hatamie, *Spectrochim. Acta Part A* **2013**, *106*, 185; c) Y. Xiang, K. Deng, H. Xia, C. Yao, Q. Chen, L. Zhang, Z. Liu, W. Fu, *Biosens. Bioelectron.* **2013**, *49*, 442.
[11] a) M. Gajendiran, Y. Jainuddin, M. Sheik, V. Elangovan, S. Balasubramanian, *J. Mater. Chem. B* **2014**, *2*, 418; b) R. Kalluru, F. Fenaroli, D. Westmoreland, L. Ulanova, A. Maleki, N. Roos, M. P. Madsen, G. Koster, W. Egge-Jacobson, S. Wilson, *J. Cell Sci.* **2013**, *126*, 3043; c) L. L. I. J. Booysen, L. Kalambo, E. Brooks, R. Hansen, J. Gilliland, V. Gruppo, P. Lungenhofer, B. Semete-Makokolela, H. S. Swai, A. F. Kotze, *Int. J. Pharm.* **2013**, *444*, 10; d) I. P. Kaur, M. K. Verma, *Int. J. Pharm.* **2011**, *1*, 110; e) G. K. Saraogi, P. Gupta, U. D. Gupta, N. K. Jain, G. P. Agrawal, *Int. J. Pharm.* **2010**, *385*, 143.
[12] A. Banu, V. Rathod, *J. Biomed. Nanosci. Nanotechnol.* **2013**, *3*, 211.
[13] a) H. Gröger, F. Gyger, P. Leidinger, C. Zurmühl, C. Feldmann, *Adv. Mater.* **2009**, *21*, 1586; b) D. H. M. Buchold, C. Feldmann, *Nano Lett.* **2007**, *7*, 3489.
[14] D. Lindsay, *Min. Soc. Am.* **1976**, 3.
[15] a) Y. Chao, P. P. Karmali, R. Mukthavaram, S. Kesari, V. L. Kouznetsova, I. F. Tsigelny, D. Simberg, *ACS Nano* **2013**, *7*, 4289; b) L. K. Bogart, A. Taylor, Y. Cesbron, P. Murray, R. Levy, *ACS Nano* **2012**, *6*, 5961.
[16] C. Gottstein, G. Wu, B. J. Wong, J. A. Zasadzinski, *ACS Nano* **2013**, *7*, 4933.
[17] J. D. López-Castro, A. V. Maraloiu, J. J. Delgado, J. J. Calvino, M.-G. Blanchin, N. Galvez, J. M. Domınguez, *Nanoscale* **2011**, *3*, 4597.
[18] A. Dube, J. L. Reynolds, W. C. Law, C. C. Maponga, P. N. Prasad, G. D. Morse, *Nanomedicine* **2014**, *10*, 831.
[19] L. Lartigue, D. Alloyeau, J. Kolosnjaj-Tabi, Y. Javed, P. Guardia, A. Riedinger, C. Pechoux, T. Pellegrino, C. Wilhelm, F. Gazeau, *ACS Nano* **2013**, *7*, 3939.
[20] Reviews: a) P. W. Goodwill, E. U. Saritas, L. R. Croft, T. N. Kim, K. M. Krishnan, D. V. Schaffer, S. M. Conolly, *Adv. Mater.* **2012**, *24*, 3870; b) N. Lee, T. Hyeon, *Chem. Soc. Rev.* **2012**, *41*, 2575.
[21] a) H. Drakesmith, A. M. Prentice, *Science* **2012**, *338*, 768; b) S. M. Santhanagopalan, G. M. Rodrigues, *Tuberculosis* **2012**, *92*, 60; c) A. K. Sharma, R. Naithani, V. Kumar, S. S. Sandhu, *Curr. Med. Chem.* **2011**, *18*, 1723; d) U. E. Schaible, S. H. Kaufmann, *Nat. Rev. Microbiol.* **2004**, *2*, 946.

Received: June 15, 2015
Revised: July 16, 2015
Published online: August 31, 2015

